

MEMS DESIGNED FOR TUNABLE CAPACITORS

Huey D. Wu, Kevin F. Harsh, Ronda S. Irwin, Wenge Zhang,
Alan R. Mickelson, and Y. C. Lee

NSF Center for Advanced Manufacturing and Packaging of
Microwave, Optical and Digital Electronics,
Department of Mechanical Engineering, and
Department of Electrical and Computer Engineering
University of Colorado, Boulder, CO 80309-0427

Joseph B. Dobsa
National Security Agency
Fort George Meade, MC 29755-6516

ABSTRACT

A new tunable capacitor based on a standard microelectromechanical systems (MEMS) technology has been demonstrated. Its unique feature was the design to use thermal actuators as indirect drives to change air gap from 2 to 0.2 μm for high-Q mm-wave capacitors. Such a drive scheme achieved a sub- μm controllability. The insertion loss of a polysilicon MEMS capacitor was measured to be -4dB at 40 GHz. Such a loss would have been better than -1dB if the polysilicon were coated with metal.

INTRODUCTION

High-Q tunable capacitors are enabling components for millimeter-wave (mm-wave) systems. As shown in Figure 1, for the tunable capacitors, there are two approaches to make high-Q components. One is a chemical approach that improves properties of ferroelectric materials. The other is a physical approach that controls the gap or area of the dielectric layer for variable capacitance. MEMS with precise, μm -level movement are ideal drives for the physical approach. A MEMS-based switching diaphragm could be used as a variable capacitor [Goldsmith et al., 1995]. The quality factor (Q)

of this component was very impressive because lossless, 2- μm air gap was used for the dielectric layer. Unfortunately, the range of this variable capacitance was limited because the top membrane could collapse onto the bottom plate when the gap height was smaller than 77% of the original level.

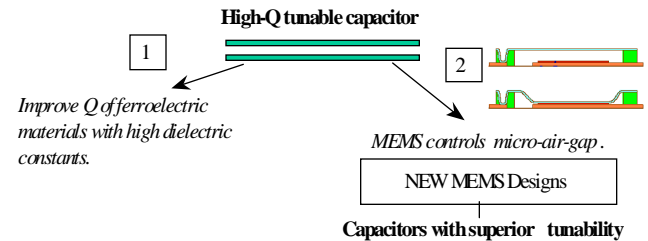


Figure 1: Two approaches for tunable capacitors

MEMS FOR TUNABLE CAPACITORS

A new MEMS component has been designed to eliminate such a limit. The key feature was the use of indirect drive instead of the electrostatic direct drive that was closely coupled with the gap variation. As shown in Figure 2a, a thermal actuator was used to control the gap of the tunable capacitor. The thermal actuator was driven by differential thermal expansions of the thick/thin polysilicon arms [Reid et al., 1997]; it bent back-and-forward to move the top plate for the gap control. Figure 2a shows the layout of

the capacitor, and Figure 2b is a SEM photo of the real component fabricated using the MCNC's MUMPS processes.

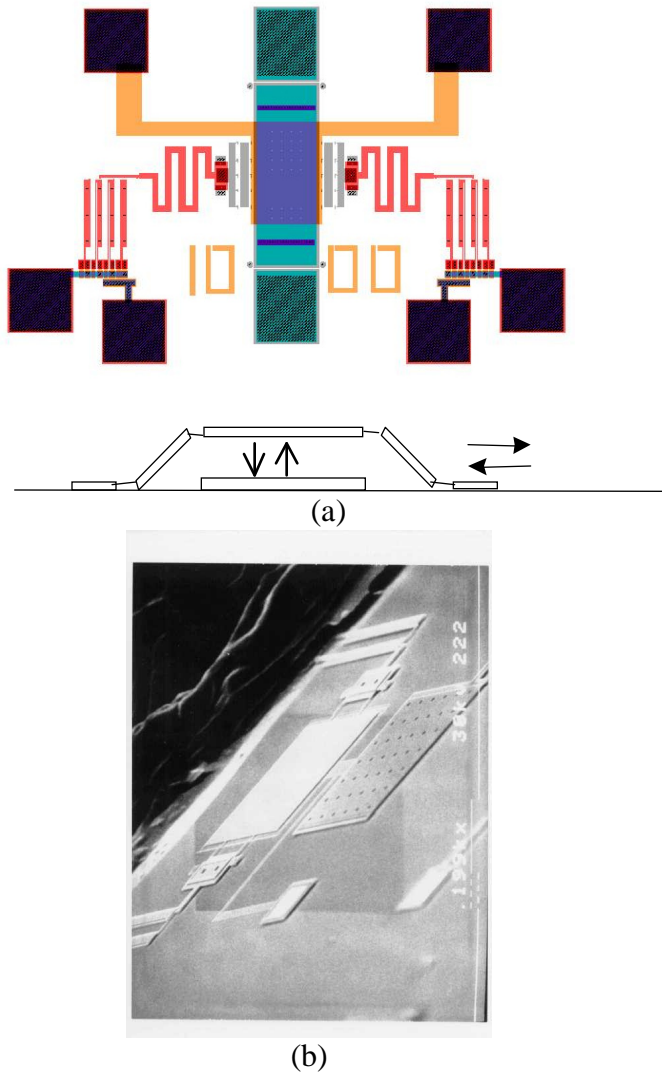


Figure 2: MEMS tunable capacitor with an indirect drive using thermal actuators.

Figure 3 presents the capacitance relative to a reference level corresponding to different applying voltages. Four data sets measured are presented with two interesting observations. The first observation is the range of the capacitance change, which achieves a very impressive level of 2.6 pF. The corresponding gap variation should be from 2 to 0.2 μ m. The second observation is the excellent repeatability and

resolution of the capacitance-vs.-voltage relationship. Small voltage changes such as 0.1 Volt result in visible capacitance variations. More importantly, all data sets repeat very well. The component could reach the same measured capacitance at the same voltage ± 0.05 Volt.

The results measured have proven the feasibility of the designed MEMS for tunable capacitors. However, enhancement was needed. In particular, the silicon had to be removed to avoid any RF interference. Figure 4 presents a new approach with a flip-chip assembly of the MEMS-on-ceramics. A SiO_2 sacrificial layer was placed between the MEMS components and the silicon; after the assembly, the silicon was removed during the release process. Figure 5 is a SEM photo of the flip-chip MEMS with the silicon removed. It should be noted that the MEMS structure was different from the one shown in Figure 2. Short MEMS were preferred for easy removal of the silicon. The measured S-parameters for two such capacitors are shown in Figures 6 and 7.

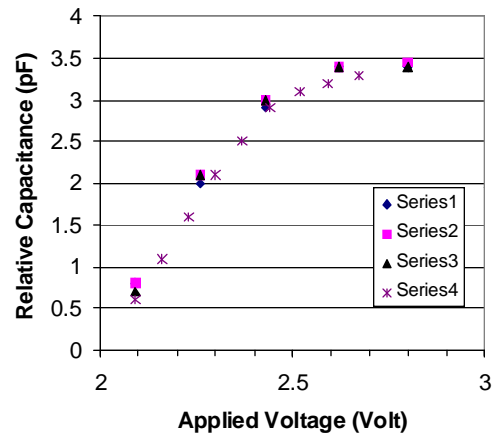


Figure 3: Measured relative capacitances

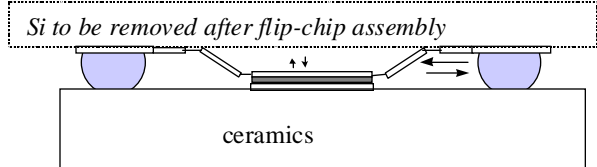


Figure 4: Flip-chip MEMS on Ceramics

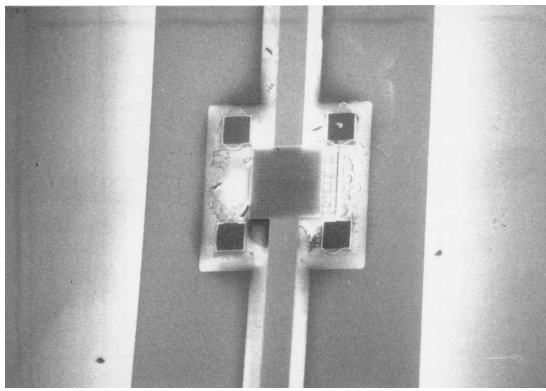


Figure 5: SEM Photo of the flip-chip MEMS bonded on coplanar test circuits

Three very encouraging results are shown in these two figures. Firstly, two different components resulted in very similar performance. The similarity proved excellent repeatability of the flip-chip assembly and the release process. Secondly, the performance was a typical one for a capacitor. The reflection dropped substantially when the impedance matched well with the 50Ω of the coplanar test circuits. Finally, the insertion loss (S_{21}) was only around -3 to -4 dB through the polysilicon MEMS. The resistance of the polysilicon was measured to be 9.2Ω . The resistance for the $500 \mu\text{m}$ square MEMS did contribute a lot to the loss. If metal, with a resistance value of 0.05Ω for the standard MCNC MEMS processes, were used for the MEMS, the loss could have been better than -1dB!

ACKNOWLEDGEMENT

This project was supported by the Department of Defense (MDA904-97-C-0320).

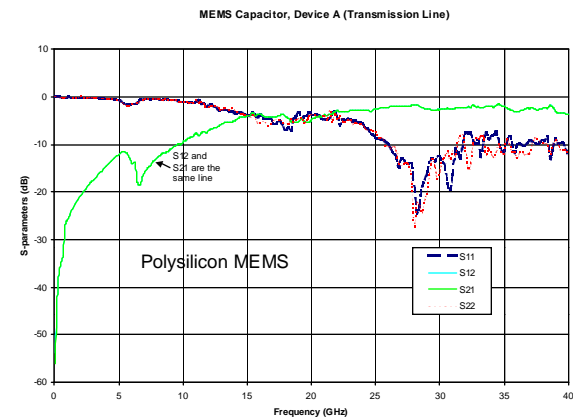


Figure 6: S-parameters for capacitor - A (polysilicon MEMS)

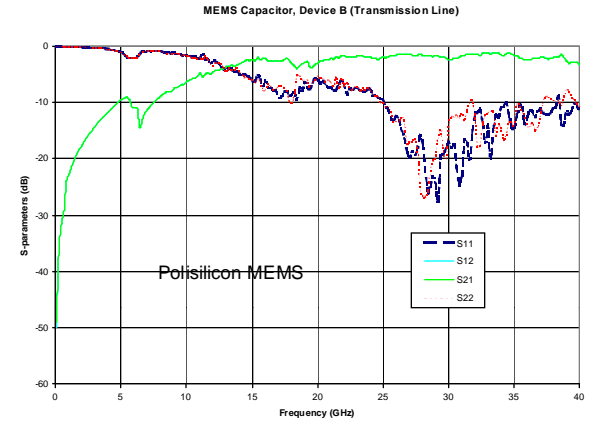


Figure 7: S-parameters for capacitor - B (polysilicon MEMS)

REFERENCES

C. Goldsmith, T.H. Lin, B. Powers, W.R. Wu, and B. Norvell, "Micromechanical Membrane Switches for Microwave Applications," 1995 IEEE MTT-S Int. Microwave Symp. Dig., pp. 91-94, May 1995.

J. R. Reid, V. M. Bright and J. H. Comtois, "Automated Assembly of Flip-Up Micromirrors," 1997 International Conference on Solid-State Sensors and Actuators, Chicago, June 16-19.